

Numerical Simulation of Solar Cell Plasmonics for Small and Large Metal Nano Clusters Using Discrete Dipole Approximation

Alok Ji · R. P. Sharma · Anju Kumari · N. K. Pathak

Received: 14 June 2013 / Accepted: 10 September 2013 / Published online: 21 September 2013
© Springer Science+Business Media New York 2013

Abstract We suggest a numerical model for nano-modified plasmonic optical structure, which facilitates photons to travel larger distances inside a thin-film silicon wafer, to enhance overall absorption in thin-film silicon solar cell. The absorption and scattering calculation is done using the discrete dipole approximation technique which is valid for both small and large-particle regimes. Relaxed geometrical topologies beyond quasi static approximation were addressed in the present model. The model gives a wide range of flexibility to optimize various parameters accurately. The model establishes that aspect ratio 0.5–0.6 and particle size of 140 nm for ellipsoidal shape are optimized parameters for efficient light trapping in 900–1,100 nm spectral range.

Keywords Surface Plasmon · Photovoltaics · Scattering Efficiency · Discrete Dipole Approximation

Introduction

Plasmonics (the interaction between electromagnetic fields and electrons in conduction band in metallic nanostructures) has become an important optical engineering tool to manipulate the solar spectrum by putting a nano-sized metal obstacle in its way to guide the photons to travel larger distances into the cell resulting in enhanced thin-film solar cell efficiency [1]. Recent years have seen a renewed interest in trapping solar energy efficiently and economically [2–4]. An electron in metal plasma oscillates when exposed to time-varying electric field. The oscillation is characterized by a resonance between fundamental frequency of oscillations of metal and

driver frequency of electric field. The conduction electrons in the presence of restoring force provided by positive charges oscillate at a frequency known as plasmon frequency [5].

Thin-film solar cells are usually 1–2- μm thick in comparison to conventional thick cell (180–300 μm) which can reduce the amount of costly and pure crystalline semiconductor used in thick solar cells and at the same time, there is reduction of the losses from minority carrier recombination due to shorter carrier diffusion paths [6–8]. The reduction of width of the film also reduces the path length of the photons in the semiconductor resulting in very poor efficiency especially in near-infrared domain (800–1,200-nm wavelength). So, extraction maximum efficiency from thin-film solar cell is incorporated with a light trapping mechanism. But unfortunately, all mechanisms introduce a loss component to the device and focus on plasmonics as a light trapping mechanism since the past few years that gives a wide range of tunability to optimize absorption within in the film.

It has been found that that the localized surface plasmon excitations can be utilized for thin-film solar plasmonics specifically to achieve guided scattering to travel longer distances in thin-film wafer. Large-sized (~ 100 nm) nanoparticles (NPs) have two resonant peaks and their relative extinction depends on whether the anisotropy is in perpendicular or parallel to the wafer. The backward scattering can be tuned to be low so that the NPs act as an anti-reflecting coating for solar PV [4, 6]. The forward and backward intensity may be compared as they are a crucial parameter for design, and for solar application, the backward scattering may be tuned to be low [7].

The realistic structure is not spherical; when fabrication of NPs is being done, it loses its sphericity so the NPs may take random structures such as ellipsoid, disc, or rectangular block; with the introduction of this kind of anisotropy, multipoles are generated followed by redshifting of the resonance [8]. The redshifting may also be observed when a NP is surrounded by

A. Ji (✉) · R. P. Sharma · A. Kumari · N. K. Pathak
Centre for Energy Studies, Indian Institute of Technology,
New Delhi 110016, India
e-mail: alokshukla@gmail.com

high-refractive index material. Fortunately, this resonance is highly tunable and we have a large number of parameters to control the width and position of the surface plasmon resonance (SPR).

In our recent paper [9], we made some preliminary estimates of enhanced efficiency due to the presence of the NPs in quasi static domain. But real estimation of resonance magnitude and its position can only be done using suitable numerical technique supported by suitable parameter space. In the present paper, we model thin-film solar cell efficiencies with dilute surface coverage of metal nanoparticles (MNPs) spread over the front surface of the cell. We wanted to go beyond quasi-static approximation to optimize the particle size, resonance width, and position, so we have used discrete dipole approximation (DDA) [10, 11] as a numerical technique to analyze large-particle size with different geometrical structures.

Method

Different geometries have been proposed for plasmonic light trapping in thin-film solar cells [12]. To model a nano-plasmonic solar cell, we assume a case where MNPs lie over thin-film Si solar cell (Fig. 1). The morphology of NPs considered in the present model are spherical, ellipsoidal (specifically prolate and oblate), and rectangular block. The presence of metalodielectric interface ensures SPR and metal of choice may be silver or gold because of lowest plasma frequency among the noble metals and their low-absorption losses when compared to other metals lying in visible domain of the solar spectrum [13]. Silver may be preferred over gold because of its low cost which suits its viability for photovoltaic application particularly at a very large scale.

The electron optical response in metal can be taken into account using suitable optical material function. The dielectric function of metal decides not only its position of surface plasmon resonance but also its shape. The dielectric function

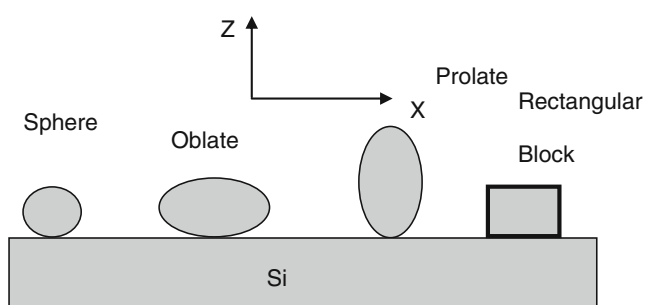


Fig. 1 Sketch of thin-film silicon solar cell structure with different shape of Ag and Au MNPs on top of a thin silicon layer

of silver (ε_p) with retardation and boundary scattering effects of electron can be written as [14–16]:

$$\varepsilon_p(\omega, a) = \varepsilon_{bulk}(\omega) + \omega_p^2 \left(\frac{1}{\omega^2 + \gamma_{bulk}^2} - \frac{1}{\omega^2 + \gamma^2(a)} \right) + i \frac{\omega_p^2}{\omega} \left(\frac{\gamma(a)}{\omega^2 + \gamma^2(a)} - \frac{\gamma_{bulk}}{\omega^2 + \gamma_{bulk}^2} \right) \quad (1)$$

Where γ_{bulk} is the damping constant of bulk silver, γ is the modified damping constant, $\varepsilon_{bulk}(\omega)$ is the bulk dielectric function of silver, ω_p is the plasma frequency, and a is the size of the particle taking volume equivalent radius. For silver, $\omega_p = 14.0 \times 10^{15}$ rad/sec. The modified damping constant may be written as:

$$\gamma = \gamma_{bulk} + A \frac{v_f}{a_{eff}} \quad (2)$$

Where $A=1$ (for isotropic scattering) and $1/\gamma_{bulk} = 31 \times 10^{-15}$ S, and $V_f = 1.39 \times 10^6$ m/s is the Fermi velocity of electrons in silver.

The Mie scattering theory is a general solution for the case of sphere in any particle size limit and its extension for the case of ellipsoid has also been calculated. But in the limit where the particle is not very small (for example $\gg 10$ nm) compared with the wavelength (for air mass (AM) 1.5 spectra) we have to calculate the scattering and absorption properties using some numerical techniques like DDA, FDTD, or FEM to consider the effects arising from retardation and radiative damping in the present model.

Discrete Dipole Approximation

DDA [10, 11, 17] is a very flexible and powerful technique for computing optical properties such as scattering and absorption by targets of arbitrary geometry. We replace the target by an array of N -point dipoles by specifying both the geometry (location \vec{r}_i of the dipoles $i=1 \dots N$) and the dipole polarizabilities $\vec{\alpha}_i$. Each entity is assigned with a dipole moment given by

$$\vec{p}_i = \alpha_i \cdot \vec{E}_{i,loc} \quad (3)$$

$$\vec{E}_{i,loc} = \vec{E}_{i,app} + \vec{E}_{i,ind} \quad (4)$$

$$\text{Where } \vec{E}_{i,app} = E_0 e^{i(\vec{k} \cdot \vec{r} - \omega t)}$$

$$\vec{E}_{i,ind} = - \sum_{j=1}^N \vec{A}_{ij} \cdot \vec{p}_j \quad (5)$$

$$\vec{A}_{ij} \cdot \vec{p}_j = \frac{e^{ikr_{ij}}}{r_{ij}^3} \left\{ k^2 \vec{r}_{ij} (\vec{r}_{ij} \times \vec{p}_j) + \frac{(1-ikr_{ij})}{r_{ij}^2} [r_{ij}^2 \vec{p}_j - 3\vec{r}_{ij} (\vec{r}_{ij} \cdot \vec{p}_j)] \right\} \tag{6}$$

$$\vec{p}_i = \alpha_i \cdot \left(\vec{E}_{i,app} - \sum_{j=1}^N \vec{A}_{ij} \cdot \vec{p}_j \right) \tag{7}$$

where \vec{r}_{ij} is the vector from the position of dipole i^{th} to dipole j the r_{ij} denotes its magnitude, and $k = |k|$

where $\vec{E}_{i,app}$ is the applied field, and $\vec{E}_{i,ind}$ is the induced field acting on the i^{th} entity due to the radiation of all the others $(N-1)$ dipoles that compose the nanoparticle [18].

From the above expression, we can calculate the set of dipole moments that mimic the optical response of the target geometry and once we know each \vec{p}_i , it is possible to obtain the light extinction and absorption cross sections using the following expressions [19–21]:

$$C_{ext} = \frac{4\pi k}{|\vec{E}_o|^2} \sum_{i=1}^n \text{Im} \{ \vec{E}_{i,inc} \cdot \vec{p}_i \} \tag{8}$$

$$C_{abs} = \frac{4\pi k}{|\vec{E}_o|^2} \sum_{i=1}^N \left\{ \text{Im} [\vec{p}_i \cdot (\alpha_i^{-1}) \cdot \vec{p}_i^*] \right\} - \frac{2}{3} k^3 |\vec{p}_i|^2 \tag{9}$$

$$C_{sca} = C_{ext} - C_{abs} \tag{11}$$

* sign is for complex conjugate.

To estimate the plasmonic effect on the thin wafer overall absorption with and without NP weighted by the AM 1.5 solar

spectrum and integrated up to the band edge of Si, The overall efficiency of the thin-film Si cell with NPs is given by [22]:

$$\eta = \frac{\int_0^{\lambda_g} I(\lambda) Q_{scat}(\lambda) \frac{\lambda}{\lambda_g} d\lambda}{\int_0^{\infty} I(\lambda) d\lambda} \tag{12}$$

where $I(\lambda)$ is the number of photons according to AM 1.5 solar spectrum [23] available, Q_{scat} is the normalized scattering cross section, and λ_g is the band edge for Si solar cell [24].

The number of photons absorbed N_{ab} in the presence of NP is given by [9]:

$$N_{ab} = [I(\lambda) \times N_p \times C_{scat} + I(\lambda) \times (1-N_p \times C_{ext}) \times A] \tag{13}$$

where N_p is the number of NPs taken for 10 % coverage area (within the dilute limit where the electromagnetic interactions among NPs is not considered) and A is the absorption fraction of 1- μm thick silicon wafer taking multiple absorption in cell into consideration. A is given by:

$$A = 1 - \left[R + \frac{T^2 R S^2}{1 - R^2 S^2} + \frac{T^2 S}{1 - R^2 S^2} \right] \tag{14}$$

where $S = e^{-\alpha x}$ (α is the absorption coefficient and $x = 1 \mu\text{m}$ is the thickness of silicon wafer), R and T are the reflection and transmission coefficients of silicon wafer, respectively.

Fig. 2 Scattering efficiency of Ag MNPs for sphere (radius $a = 70 \text{ nm}$), oblate ($h_x = h_y = 70 \text{ nm}$ and $h_z = \text{aspect ratio} \times h_x$ where aspect ratio = 0.5), prolate ($h_x = h_y = 70 \text{ nm}$ and $h_z = \text{aspect ratio} \times h_x$ where aspect ratio = 0.5) and rectangular solid (1:2:2 and $a = 70 \text{ nm}$); as a function of the wavelength of the incident light

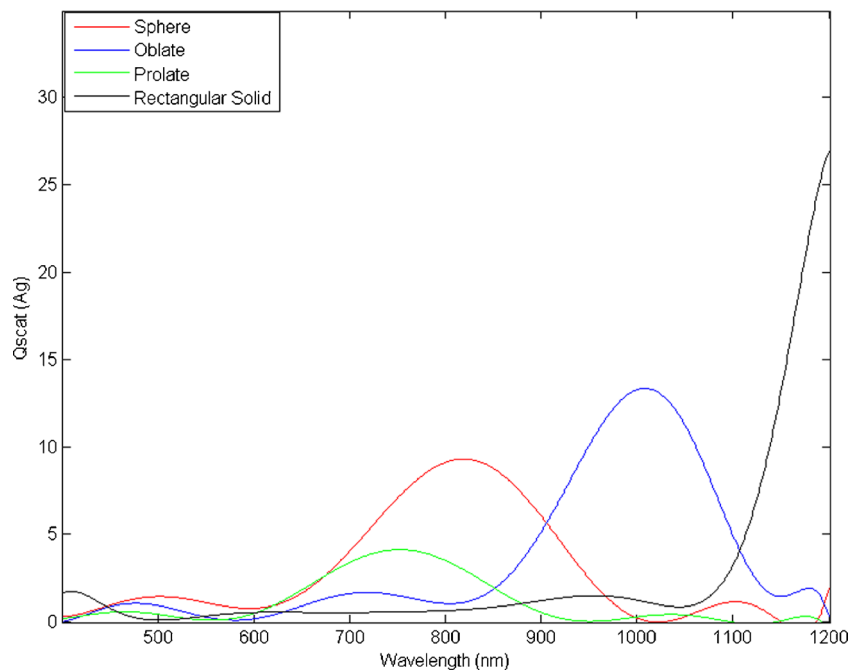
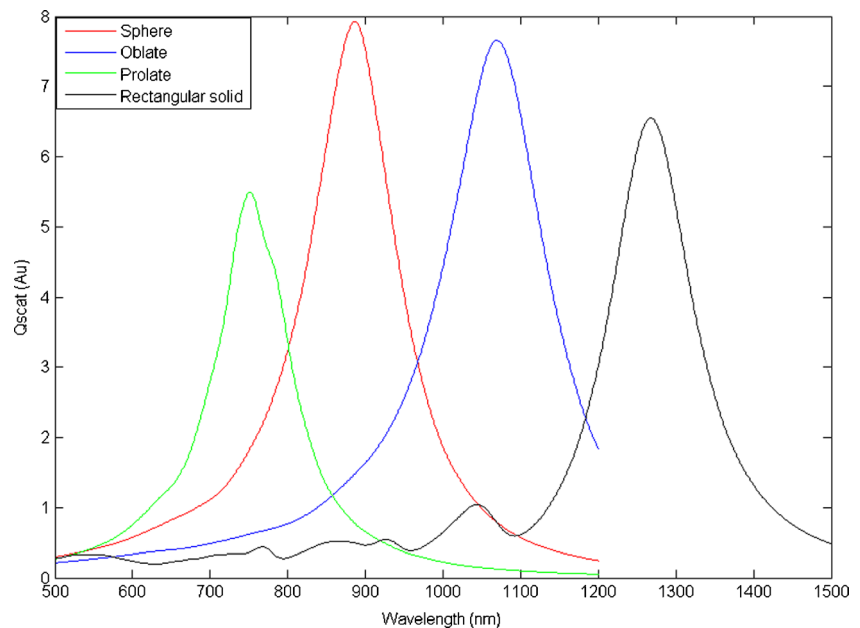


Fig. 3 Scattering efficiency of Au MNPs for sphere (radius $a = 70$ nm), oblate ($hx = hy = 70$ nm and $hz = \text{aspect ratio} \times hx$ where aspect ratio = 0.5), prolate ($hx = hy = 70$ nm and $hz = \text{aspect ratio} \times hx$ where aspect ratio = 0.5) and rectangular solid (1:2:2 and $a = 70$ nm); as a function of the wavelength of the incident light



Results and Discussion

The numbers of dipoles used for calculations of optical properties were nearly $\sim 65,500$ for better results and grid size for wavelength was 1 nm. The bulk properties of Ag and Au were used from reference [13]. Two incident polarization state E_{0x} and E_{0y} have both been considered and the overall scattering calculation is based on the average of the two polarization states.

The tuned NP SPR scattering in a targeted wavelength domain is a tool to manipulate incident light and guide it along

the thin Si film. The path length of the light in the semiconductor increases the enhancement of the absorption of photons and efficiency of cell. Figures 2 and 3 show the Q_{scat} for different shapes of Au and Ag NPs; sphere (70 nm), oblate (70 nm and aspect ratio 0.5), prolate (70 nm and aspect ratio 0.5) and rectangular solid ($l/b/h = 1:2:2$ and effective radius = 70 nm).

If we consider a sphere which can be explained by a dipolar model, a single peak is observed, whereas other structures having multipolar scattering may give rise to multiple peaks; for example, in ellipsoid, double peaks exists. The peaks may

Fig. 4 Scattering efficiency of an oblate ($hx = hy = 70$ nm and $hz = \text{aspect ratio} \times hx$ where aspect ratio = 0.5) Ag nanoellipsoid as a function of wavelength with different values of $hx = 40, 50, 60, 70,$ and 80 nm

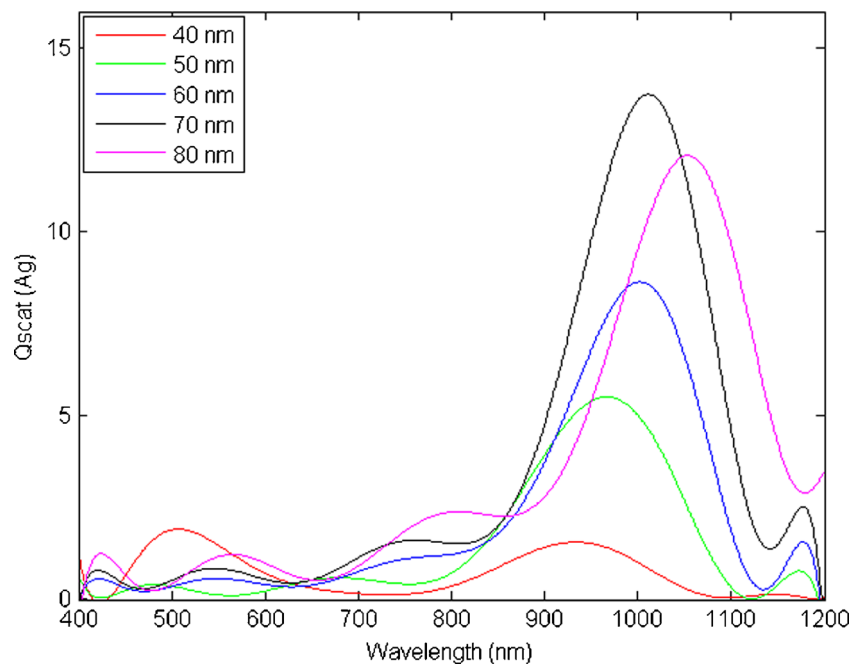
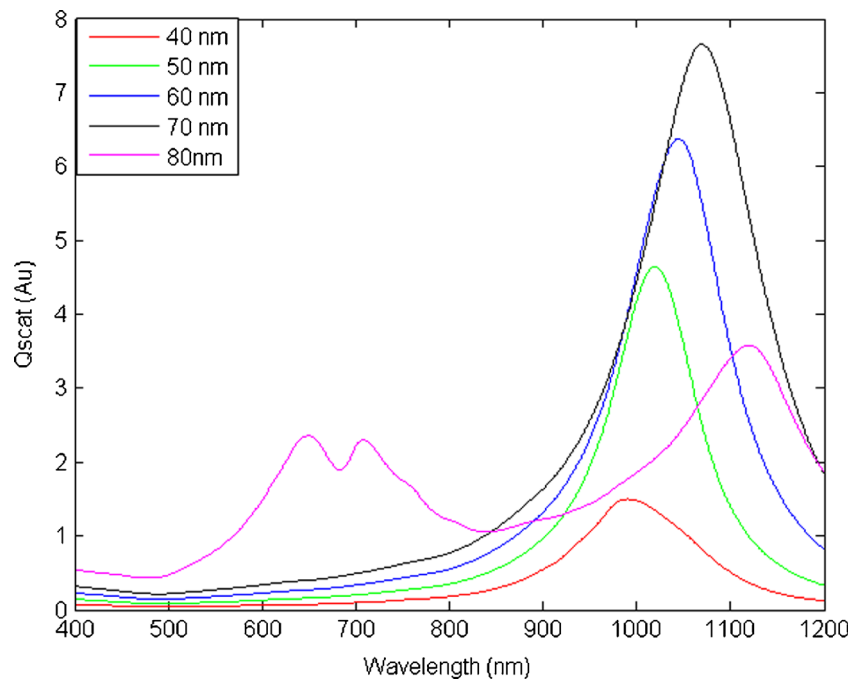


Fig. 5 Scattering efficiency of an oblate ($h_x=h_y=70$ nm and $h_z =$ aspect ratio $\times h_x$ where aspect ratio=0.5) Au nanoellipsoid as a function of wavelength with different values of $h_x=40, 50, 60, 70,$ and 80 nm



result in broad band scattering and may be very useful for solar cell applications. To understand the existence of multiple peaks physically, let's take the example of spheroidal NPs. In spheroidal NPs, there are two different resonant peaks of different intensities. The relative intensity depends on the elongation in a particular direction and hence, finally, on dipolar length. Figures 2 and 3 points out high degree of tunability of scattering profile as far as symmetry is concerned, for example, blue shift as we go from the rectangular solid to the more symmetrical

sphere case. So, we conclude from Figs. 2 and 3 that different unsymmetrical structures (for example ellipsoid (prolate or oblate), rectangular solid, etc.) may be useful for our purpose as compared to nanosphere to facilitate resonant scattering in near band gap region of Si (around 1,100 nm). We have calculated Q_{scat} for oblate Nano ellipsoid (Figs. 4 and 5) for the cases of Ag and Au, respectively. It is also observed from Figs. 4 and 5 that there is a red shift of scattered spectrum as the size increases from 40–80 nm for both Ag and Au NPs. The

Fig. 6 Scattering efficiency of an oblate Ag nanoellipsoid as a function of the wavelength of the incident light with different aspect ratios of 0.4, 0.5, and 0.6 keeping $h_x=70$ nm

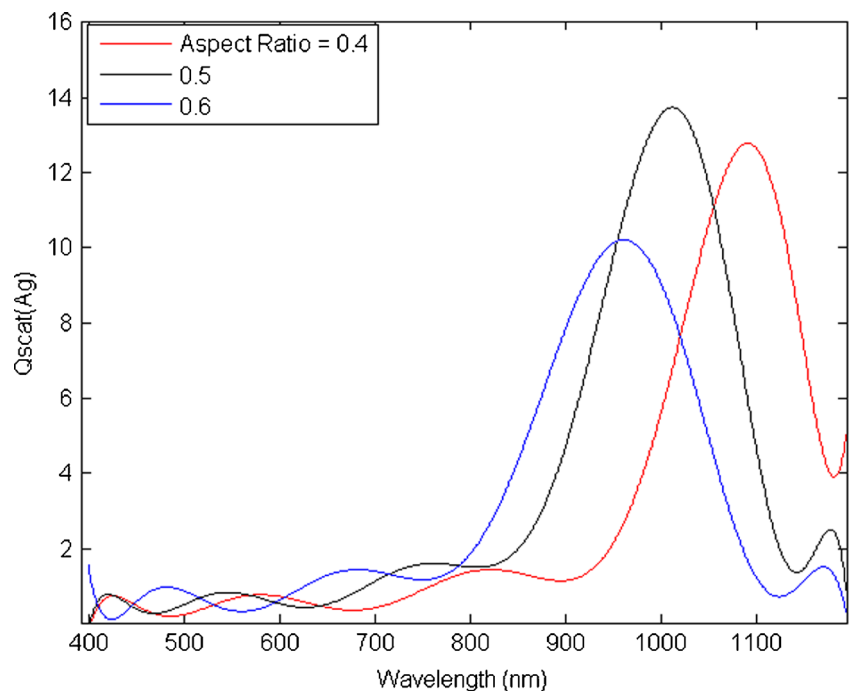
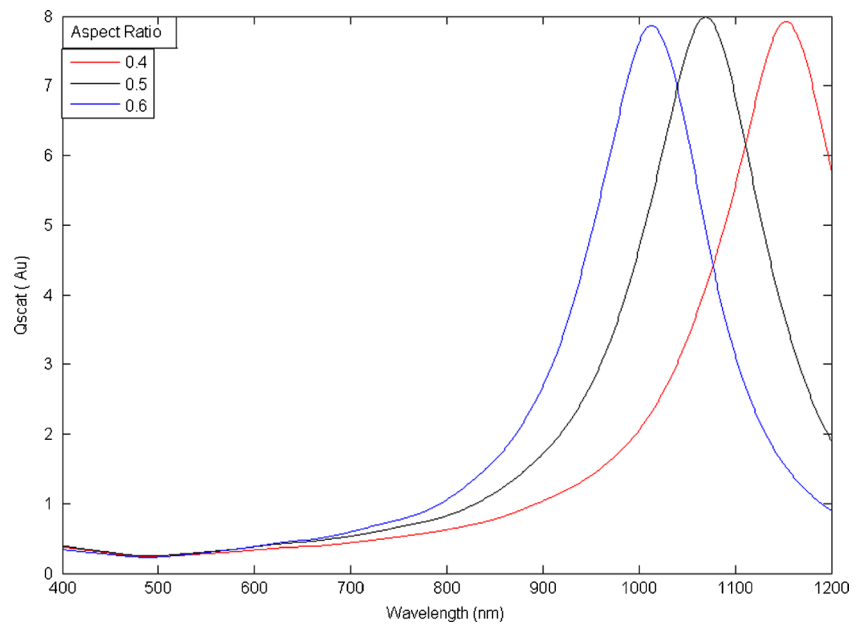


Fig. 7 Scattering efficiency of an oblate Au nanoellipsoid as a function of the wavelength of the incident light with different aspect ratios of 0.4, 0.5, and 0.6 keeping $h_x=70$ nm

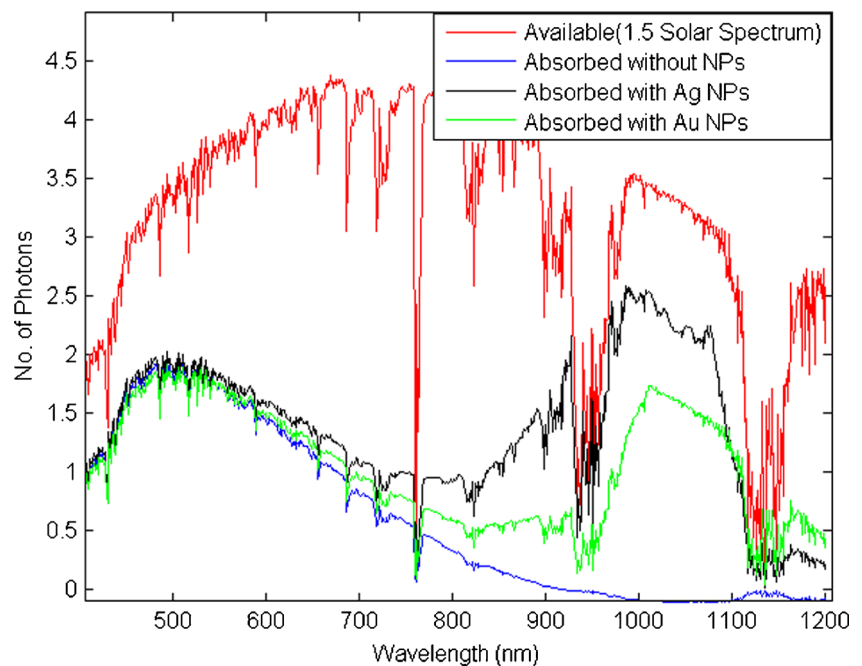


scattering efficiency increases with the increase in size of the NPs as shown in Figs. 4 and 5. Small particles are good absorbers and big particles are good scatterers when compared to wavelength. The scattering at resonance may be tuned and is thus a tool to harvest light in solar cell. In large-particle domain (for example 80-nm radius in present case), however, increasing the particle size leads to increased retardation effects and higher order multipole excitation modes, which decrease the efficiency of the scattering process.

In the light of suitability discussed above, let us discuss how silver and gold nanoellipsoids give a broad tunability range using various parameters to suit its application in light trapping.

We have plotted optical absorption and scattering from silver and gold nanoellipsoid (with $h_x=70$ nm and an aspect ratio of 0.5 where h_x , h_y , and h_z are ellipsoid semi-axes) as calculated from Figs. 4 and 5. We can tailor the NP so that optical absorption is very low as compared to scattering in the desired range of wavelength within the NPs. The more the scattering from nanoellipsoid, the more the absorption into the solar cell; hence, the better the efficiency of the solar cell. This has been proved experimentally that increased scattering results in higher photon absorption, which results as increased photocurrent. During the fabrication of the device, the actual situation will be randomly oriented ellipsoids as it is nearly impossible to

Fig. 8 Absorption of photons in a thin silicon film with and without NPs (oblate Ag and Au) with $h_x=70$ nm and aspect ratio=0.5



deposit them in a specific orientation. The influence of aspect ratio (0.4, 0.5, and 0.6) on the light scattering efficiency of oblate silver and gold Nano ellipsoid ($hx=70$ nm) is demonstrated in Figs. 6 and 7. Depending on the direction of the incident field and the elongation of NPs along an axis, the scattering resonance may get shifted to a particular wavelength. SPR blue shifts with the increasing aspect ratio; we achieve the resonance at the band gap wavelength of Si for the aspect ratio value of 0.5. Spheroidal NP exhibits double resonances, corresponding to oscillations of its conduction electrons along the major or minor axis, respectively. The resonance corresponding to major axis having higher dipole moment is responsible for greater red shift than corresponding to minor one. Thus, plasmon resonances can be tuned to lower frequency using different parameters in the presence of high-refractive index to red-wavelength region.

The overall effect of resonant scattering results in high absorption in near-infrared domain of the AM 1.5 global spectrum which can be realized from Fig. 8, where absorption in cell weighted by $I(\lambda)$ and Q_{scat} were calculated (using Eq. 13) and for bare Si cell multiple absorption in thin wafer was considered. Both were plotted against the wavelength to observe the overall affect due to Ag and Au. If we consider that after scattering, all of the photons are guided into the thin-film and they observe increased path length, we see that red response of the cell increases dramatically.

Conclusion

The present numerical technique gives the flexibility and wide scope to optimize all key parameters associated with SPR. The resonance peaks, position, width, and efficiency have been discussed and optimized. The study shows that the extensive tunability, high-forward scattering, and optical path length enhancement are potentially promising to attain low-cost efficient thin-film solar cells. The physics involving shape, material, and geometry attracts readers from different fields for variety of applications.

Finally, our results suggest that proper adjustment of the parameters influencing the resonance lead to the new generation

of highly efficient SPR-enhanced Si solar cells as sources of cheap and environmentally friendly renewable energy. The thin-film cell will have almost the same efficiency as compared to thick wafer which is a very promising indication towards cost reduction.

Acknowledgments This research is partially supported by DST (India).

References

- Spinelli P, Ferry VE, van de Groep J, van Lare M, Verschuuren MA, Schropp REI, Atwater HA, Polman A (2012) *J Opt* 14:024002
- Polman A et al (2012) *J Opt* 14:024002
- Green MA (2004) *Sol Energy* 76:3
- Mokkapati S, Catchpole KR (2012) *J Appl Phys* 112:101101
- Kreibig U, Vollmer M (1995) *Optical properties of metal clusters*. Wiley, New York
- Pillai S, Catchpole KR, Trupke T, Green MA (2007) *J Appl Phys* 101:093105
- Atwater HA, Polman A (2010) *Nature Mater* 9:205
- Akimov YA, Ostrikev K, Li EP (2009) *Plasmonics* 4:107
- Ji Alok, Sangita, Sharma RP (2012) *J Phys D Appl Phys* 45:275101
- Purcell M, Pennypacker CR (1973) *Astrophys J* 186:705
- Draine BT, Flatau PJ (1994) *J Opt Soc Am* 11(4)
- Paris A, Vaccari A, Lesina AC, Enrico S, Calliari L (2012) *Plasmonics* 7:525
- Johnson PB, Christy RW (1972) *Phys Rev B* 6:4370
- Hu L, Chen X, Chen G (2008) *J Comput Theor Nanosci* 5:2096
- Noguez C (2007) *J Phys Chem C* 111:3806
- Maier S (2007) *Plasmonics: fundamentals and applications*. Springer, Berlin
- Draine BT, Flatau PJ User guide to the discrete dipole approximation code DDSCAT 7.2, available at <http://arxiv.org/abs/1202.3424>. Accessed 17 Sep 2013
- Landau L, Lifshitz E (1960) *Electrodynamics of continuous media*. Ergamon, London
- Draine BT, Flatau PJ (2008) *J Opt Soc Am* 25:2693
- Draine BT, Flatau PJ (2012) *Opt Express* 20:1247
- Bohren CF, Huffman DR (1998) *Absorption and scattering of light by small particles*. Wiley, New York
- Shockley W, Queisser H (1961) *J Appl Phys* 32:510
- AM1.5 Spectra, American Society for Testing and <http://redc.nrel.gov/solar/spectra/am1.5/>. Accessed 17 Sep 2013
- <http://www.pveducation.org/pvcdrom/appendicies/optical-properties-of-silicon>. Accessed 17 Sep 2013